Original Article

Phenotype Variability in Czech Patients Carrying *PAX6* Disease-Causing Variants

(aniridia / ptosis / congenital cataract / uveal coloboma / *PAX6* / novel variant / exon trapping)

J. MORAVIKOVA[1], Z. KOZMIK[2], L. HLAVATA[1], M. PUTZOVA[3], P. SKALICKA[1,4], M. MICHAELIDES[5,6], F. MALINKA[1,7], L. DUDAKOVA[1], P. LISKOVA[1,4]

[1]Research Unit for Rare Diseases, Department of Paediatrics and Inherited Metabolic Disorders, [4]Department of Ophthalmology, First Faculty of Medicine, Charles University and General University Hospital in Prague, Czech Republic
[2]Department of Transcriptional Regulation, Institute of Molecular Genetics, Czech Academy of Sciences, Prague, Czech Republic
[3]Biopticka laborator s.r.o., Pilsen, Czech Republic
[5]UCL Institute of Ophthalmology, University College London, London, UK
[6]Moorfields Eye Hospital NHS Foundation Trust, London, UK
[7]Department of Computer Science, Czech Technical University in Prague, Czech Republic

Abstract. The aim of this study was to report *PAX6* disease-causing variants in six Czech families, to describe the associated phenotypes, and to perform functional assessment of the splice site variants. Detailed ophthalmic examination was performed. The *PAX6* coding region was directly sequenced in three probands. Two probands were analysed by exome sequencing and one by genome sequencing. The effect of two variants on pre-mRNA splicing was evaluated using an exon trapping assay. Six different heterozygous *PAX6* variants were identified, with c.111_120del and c.1183+1G>T being novel. Both c.1183+1G>T and c.1032+1G>A were proved to cause aberrant splicing with exon skipping and subsequent frameshift. The phenotypic features were variable between and within families. One individual, aged 31 years, presented with mild unilateral ptosis accompanied by aniridia in the right eye, partial aniridia in the left eye, and bilateral congenital cataracts, without marked foveal hypoplasia. Bilateral microcornea, partial aniridia, congenital cataracts, and a large posterior segment coloboma were found in another proband, aged 32 years. One child, aged 8 years, had bilateral high myopia, optic nerve colobomas, anterior polar cataracts, but no iris defects. Another individual, aged 46 years, had bilateral congenital ptosis, iris hypoplasia, keratopathy with marked fibrovascular pannus, anterior polar cataract, and foveal hypoplasia combined with impaired glucose tolerance. However, his daughter, aged 11 years, showed classical features of aniridia. Our study extends the genetic spectrum of *PAX6* disease-causing variants and confirms that the associated phenotypic features may be very broad and different to the 'classical' aniridia.

Received June 4, 2020. Accepted August 19, 2020.

This work was supported by AZV 17-30500A. Institutional support was provided by UNCE 204064 and PROGRES Q26 programmes of Charles University. J. M. was supported by GAUK 250713/82318/2018 and SVV 260367/2017. M. M. is supported by grants from the National Institute for Health Research Biomedical Research Centre at Moorfields Eye Hospital NHS Foundation Trust and UCL Institute of Ophthalmology.

Corresponding author: Lubica Dudakova, Research Unit for Rare Diseases, Department of Paediatrics and Inherited Metabolic Disorders, Ke Karlovu 455/2, 128 08 Prague 2, Czech Republic. e-mail: lubica.dudakova@lf1.cuni.cz.

Abbreviations: ACMG – American College of Medical Genetics and Genomics, *AMLX/Y* – amelogenin gene on X/Y chromosome, BCVA – best-corrected visual acuity, BWA – Burrows Wheeler Aligner, CADD – combined annotation-dependent depletion, D – dioptre, DBD – DNA-binding domain, DMEM – Dulbecco's Modified Eagle's Medium, GATK – genome analysis tool kit, HD – homeodomain, LE – left eye, LNK – linker region, PD – paired domain, RE – right eye, SD-OCT – spectral domain optical coherence tomography, STR – short tandem repeat, TAD – transactivation domain.

Introduction

Aniridia (MIM #106210) is a rare congenital pan-ocular disorder with an incidence ranging from 1 : 40,000 to 1 : 96,000 (Lim et al., 2017). The characteristic feature of aniridia is complete or partial loss of the iris. Foveal hypoplasia is also usually present, leading to nystagmus and reduced visual acuity, which can be further complicated by optic nerve hypoplasia in some pa-

tients (Mayer et al., 2003; Hingorani et al., 2009; Netland et al., 2011). Later in life, aniridia is frequently associated with keratopathy, glaucoma, and presenile cataract (Valenzuela and Cline, 2004). Some cases have been reported to also have congenital cataract, congenital ptosis, microcornea, microphthalmia, sclerocornea, posterior segment coloboma, and high myopia (Gronskov et al., 1999; Dansault et al., 2007; Hewitt et al., 2007; Jin et al., 2012; Lim et al., 2012; Miyake et al., 2012; Goolam et al., 2018). Clinical presentation, including the degree of visual impairment, can significantly vary both within and between families (Gronskov et al., 1999; Malandrini et al., 2001). Rarely, behavioural abnormalities such as developmental delay have been observed (Malandrini et al., 2001; Graziano et al., 2007; Chien et al., 2009). The *PAX6* aniridia syndrome may also be associated with a variety of systemic findings, including hormonal, metabolic, gastrointestinal, genitourinary, and neurologic abnormalities (Lim et al., 2017).

Aniridia is inherited as an autosomal dominant trait in two thirds of patients; the rest of cases appear to be sporadic caused by variants occurring *de novo* (Prosser and van Heyningen, 1998; Samant et al., 2016). The disease is known to be caused by sequence variants in the paired box 6 (*PAX6*) gene, which encodes a transcriptional regulator involved in oculogenesis and other developmental processes of the brain, olfactory system and pancreas (Grindley et al., 1995; Hanson and Van Heyningen, 1995; Ton et al., 1991; Robinson et al., 2008). Classical aniridia is caused by *PAX6* haploinsufficiency, i.e., loss of function of one allele, resulting in a 50% reduction of overall activity (Prosser and van Heyningen, 1998). *PAX6* missense variants may mimic haploinsufficiency, but are more commonly associated with milder phenotypes such as partial aniridia, isolated foveal hypoplasia or optic disc malformation (Williamson et al., 2020).

Deletions that include *PAX6* and Wilms tumour 1 (*WT1*) genes are associated with the WAGR syndrome (MIM #194072), in which affected children have two or more of the following symptoms: Wilms tumour, aniridia, genital anomalies, and mental retardation (Miller et al., 1964; Gronskov et al., 2001). Rarely, aniridia-like abnormalities can be caused by pathogenic variants in two other transcription factors, forkhead-related transcription factor (*FOXC1*) or paired like homeodomain 2 (*PITX2*) (Samant et al., 2016).

In this study we report detailed clinical and molecular genetic findings in Czech patients with aniridia, including rare phenotypic presentations and functional assessment of the effect of two splicing variants.

Material and Methods

Participants and clinical examination

The research described in this study was conducted in accordance with the Declaration of Helsinki, and institutional ethics committee approval was obtained prior to the start of the study. Six unrelated Czech probands and their available family members were included.

Standard ocular examination was performed at the Department of Ophthalmology, First Faculty of Medicine, Charles University and General University Hospital in Prague. Best-corrected visual acuity (BCVA) using Snellen charts (shown in decimal values) and intraocular pressure were measured. Anterior segment and macular architecture were assessed with spectral domain optical coherence tomography (SD-OCT) (Spectralis; Heidelberg Engineering GmbH, Heidelberg, Germany).

Molecular genetic analysis

Genomic DNA was isolated from peripheral blood using Gentra Puregene™ Blood Kit (Qiagen, Hilden, Germany) or saliva samples using Oragene Saliva Collection and DNA extraction kit (Genotek, Ottawa, Canada) according to the manufacturer's instructions.

In three probands from Families 2, 5 and 6 (Fig. 1), the entire coding region of *PAX6* and flanking introns was bidirectionally analysed by conventional Sanger sequencing in the 3500 Series Genetic Analyzer (Applied Biosystems, Foster City, CA). Primer sequences and reaction conditions used for PCR and direct sequencing are listed in Table 1, NM_000280.4 was taken as the reference sequence. Sanger sequencing was also used for segregation analysis within the families.

Three probands were subjected to massive parallel sequencing. Sequencing libraries were generated for the proband from Family 3 using SureSelect Human XT kit (Agilent, Santa Clara, CA) and for the proband from Family 4 using Agilent SureSelect Human All Exome V6 capture kit. The proband from Family 1 underwent genome sequencing. The sequencing library was generated using Truseq Nano DNA HT Sample Prep Kit (Illumina, San Diego, CA) with a 350 bp target insert size. Libraries were sequenced with 2 × 150 bp paired-end reads in Illumina machines HiSeq4000 (proband 3), Novaseq6000 (proband 4) and HiSeq X Ten (proband 1). Reads were aligned to the GRCh37/hg19 human reference sequence with Burrows Wheeler Aligner (BWA) (Li and Durbin, 2009). Variant calling was performed with Genome Analysis Tool Kit (GATK, Broad institute, Cambridge, MA) HaplotypeCaller (version 4.0.1.2) (McKenna et al., 2010). Variants were annotated using ANNOVAR (Wang et al., 2010).

The frequency of the identified variants was mined from the Genome Aggregation Database (gnomAD v2.1.) showing data from 125,748 exome and 15,708 genome sequences from unrelated individuals (accessed 4/2020) (Karczewski et al., 2020). Population-specific frequency (3,930 Czech control chromosomes) was provided by the National Center for Medical Genomics (http://ncmg.cz/en). Given the rarity of aniridia, only variants with minor allele frequency ≤ 0.001 were evaluated for potential pathogenicity. These were further cross-referenced with the literature and the *PAX6* LOVD

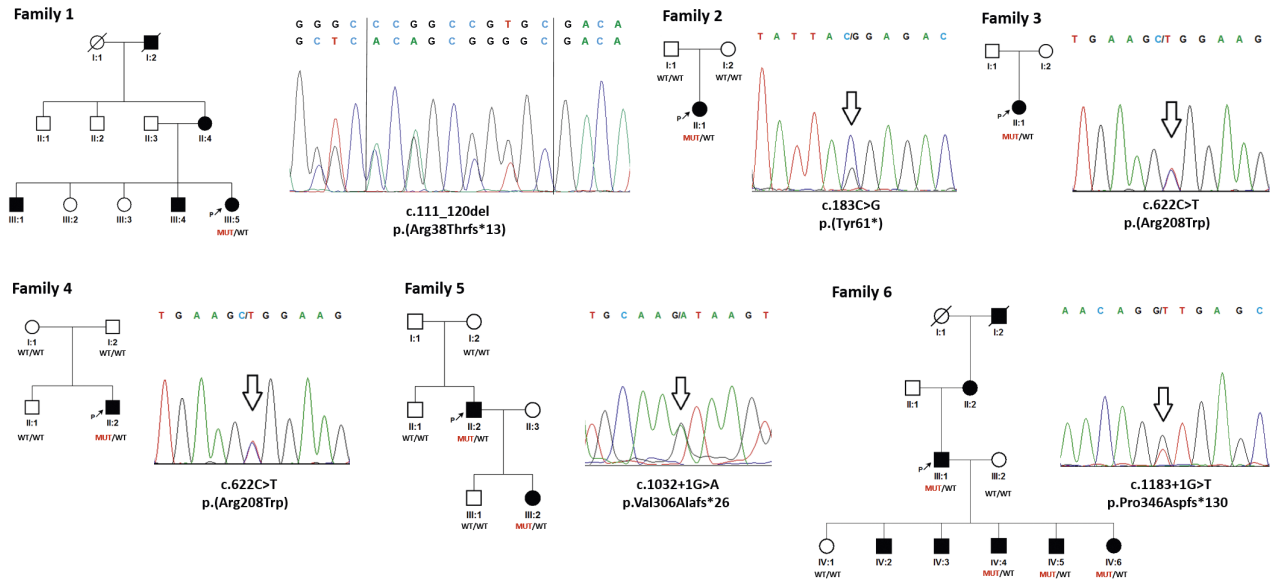

Fig. 1. Pedigrees of the families studied and sequence chromatograms of the identified variants
In Families 2 and 4, the *de novo* origin was confirmed by parental testing. WT – wild type, MUT – mutant.

Table 1. Primers and conditions used

Primer	Sequence (5'→ 3')	Annealing temperature	Product length
PCR and direct sequencing of the *PAX6* gene coding regions			
Ex4 FWD	CCCAAGAGGTTGAGTGGATCA	60 °C	387 bp
Ex4 REV	CGAGAAGAGCCAAGCAAACG		
Ex5 FWD	CTGGTGGTCCTGTTGTCCTT	60 °C	446 bp
Ex5 REV	ATGAAGAGAGGGCGTTGAGA		
Ex6 FWD	GGGCTACAAATGTAATTTTAAGAA	55 °C	509 bp
Ex6 REV	AGAGAGGGTGGGAGGAGGTA		
Ex7 FWD	GAGCTGAGATGGGTGACTG	55 °C	300 bp
Ex7 REV	GAGAGTAGGGGACAGGCAAA		
Ex8 FWD	TCAGGTAACTAACATCGCA	55 °C	719 bp
Ex8 REV	GTTGACTGTACTTGGAAGAA		
Ex9 FWD	AGGTGGGAACCAGTTTGATG	60 °C	311 bp
Ex9 REV	CATGGCAGCAGAGCATTTAG		
Ex10 FWD	GCTAAATGCTCTGCTGCCAT	60 °C	329 bp
Ex10 REV	AGAGTGAGAGTCAGAGCCCG		
Ex11 FWD	CACCACACCGGGTAATTTGAA	60 °C	329 bp
Ex11 REV	AAGCTCTCAAGGGTGCAGACA		
Ex12 FWD	GAGGCTTGATACATAGGC	55 °C	458 bp
Ex12 REV	CCATAAGACCAGGAGATT		
Ex13 FWD	TCCATGTCTGTTTCTCAAAGG	60 °C	220 bp
Ex13 REV	TCAACTGTTGTGTCCCCATAG		
Exontrap assay			
c.1032+1G>A FWD	TTTCCTAGAGACAGAGGTGCTTG	60 °C	828 bp
c.1032+1G>A REV	CCCACCACCACCCAACATTAT		
c.1183+1G>T FWD	TGGCAACCATCTAGCTGGACA	60 °C	664 bp
c.1183+1G>T REV	TGCAGTCTCAGGCCTTGTCTT		
Direct sequencing of plasmid insert and cDNA			
Exontrap PCR-2	GATCTGCTTCCTGGCCC	60 °C	
Exontrap PCR-r3	GGCACTGGAGGTGGC		
TOPO M13 REV	CAGGAAACAGCTATGAC	60 °C	
TOPO M13 FWD	CTGGCCGTCGTTTTAC		

Table 2. Results of prediction tools evaluating the PAX6 missense variant c.622C>T; p.(Arg208Trp)

SIFT	PolyPhen2	MutPred2	Mutation Taster	SNP&GO	Provean	CADD score
Disease	Disease	0.783	Disease	Disease	Disease	29.4

Abbreviations: SIFT – Sorting Intolerant from Tolerant, PolyPhen2 – polymorphism phenotyping v2, Provean – Protein Variation Effect Analyser, CADD – combined annotation-dependent depletion.
CADD score > 20 predicts that a variant is highly deleterious. As for MutPred2, an overall probability score > 0.5 was considered as probably disease-causing and a score > 0.75 was considered as disease-causing.

Predictions in Tables 2 and 3 were obtained using these web resources:
SNP&GO: http://snps.biofold.org/snps-and-go/snps-and-go.html
PolyPhen2: http://genetics.bwh.harvard.edu/pph2/
MutPred2: http://mutpred.mutdb.org/
NetGene2: http://www.cbs.dtu.dk/services/NetGene2/
PROVEAN and SIFT: http://provean.jcvi.org/index.php
MutationTaster: http://www.mutationtaster.org/
HSF3 and MaxEntScan: http://www.umd.be/HSF3/HSF.shtml
NNSPLICE: http://www.fruitfly.org/seq_tools/splice.html

database (http://grenada.lumc.nl/LSDB_list/lsdbs/PAX6, accessed 5/2020). The pathogenicity of missense variants and variants potentially affecting splicing was predicted using six and four different software tools, respectively (Table 2). Final classification of the detected variants was based on the evidence categories outlined by the American College of Medical Genetics and Genomics (ACMG) using an online tool (Richards et al., 2015; Kleinberger et al., 2016).

Paternity and maternity testing was performed in parents of the probands from Families 2 and 4 using AmpFLSTR Identifiler Plus PCR Amplification Kit (Thermo Fisher Scientific, Paisley, UK), which provides analysis of 15 different STR (short tandem repeat) loci, and also with the AMLX/Y test (McKenna et al., 2010).

Exon trapping assay

Exontrap cloning vector pET01 (MoBiTec, Goettingen, Germany) was used to determine the effect of variants residing in intron-exon boundaries on pre-mRNA splicing. Genomic DNA of affected individuals was used as a template for PCR reactions. In one proband exons 10, 11 with adjusting introns including a whole intron 10, in another proband exon 12, and their flanking intronic sequences were amplified by primers listed in Table 1. PCR amplicons representing a mix of wild-type and variant alleles were isolated from the gel, cloned into plasmid vector pCR-Blunt II-TOPO (Thermo Fisher Scientific) and directly sequenced. Plasmid clones identified as carrying either the wild-type or variant allele were digested with *Bam*HI and *Not*I and fragments were inserted into *Bam*HI/*Not*I-digested pET01. Human embryonic kidney HEK293T cells (ATCC, Manassas, VA) were cultured in DMEM (Dulbecco's Modified Eagle's Medium; Thermo Fisher Scientific) supplemented with 10% foetal bovine serum in a 37 °C incubator with 5% CO_2. pET01 vectors with the wild-type or variant sequence were transfected into HEK293T cells using FuGENE HD transfection reagent (Promega, Madison, WI). Forty-eight hours after transfection, total RNA was isolated from the cells by TRIzol reagent (Thermo Fisher Scientific) and mRNAs reverse transcribed using SuperScript VILO cDNA Synthesis Kit (Thermo Fisher Scientific). cDNA was amplified by primer pairs complementary to vector-derived exons present in the Exontrap plasmid pET01 (Table 1) and PCR products were sequenced.

Results

Molecular genetic analysis

Fifteen individuals from six families were clinically examined. Five different *PAX6* variants in a heterozygous state were identified: c.111_120del, c.183C>G, c.622C>T, c.1032+1G>A, c.1183+1G>T (Fig. 1), two being novel. All five variants were classified according to the ACMG recommendations as pathogenic.

The c.111_120del identified in Family 1 was a previously unreported frameshift variant, predicted to cause protein truncation p.(Arg38Thrfs*13). The c.183C>G found in the proband from Family 2 results in premature insertion of a stop codon, p.(Tyr61*). This variant has been previously reported in one sporadic case with aniridia (Perez-Solorzano et al., 2017). As it was not present in either parent and paternity testing was performed, we have considered it to be *de novo*.

The c.622C>T; p.(Arg208Trp) identified in Families 3 and 4 has been previously observed in three other families with aniridia spectrum disorder (Hanson et al., 1993; Goolam et al., 2018). The lack of a family history and results of paternity testing in Family 4 were suggestive of *de novo* origin. All six prediction tools used evaluated the c.622C>T as disease-causing (Table 2).

Both c.1032+1G>A and c.1183+1G>T present in Family 5 and 6, respectively, were evaluated by prediction tools as disrupting splicing (Table 3). The variant c.1032+1G>A has been previously observed in two probands with aniridia (Jordan et al., 1992; Malandrini et al., 2001), whereas c.1183+1G>T is novel. Segregation analysis of the two changes within the families supported their pathogenicity (Fig. 1). To experimentally validate and characterize their effect on splicing, an exon trapping assay was performed. The variant c.1032+1G>A led to skipping of exon 11 from the mRNA sequence (Fig. 2B), with a predicted effect of premature stop co-

Table 3. Results of prediction tools evaluating two variants located in PAX6 canonical splice sites

Mutation	HSF3			NetGene2	NNSPLICE			MaxEntScan		
	WT	MUT	Variation score	Effect of the mutated allele	WT	MUT	Variation score	WT	MUT	Variation score
c.1032+1G>A	89.42	62.59	−30%	Loss of splice site	1.00	<0.4	−100%	10.08	1.9	−81.15%
c.1183+1G>T	96.67	69.83	−27.76%	Loss of splice site	1.00	<0.4	−100%	9.6	1.1	−88.54%

Abbreviations: HSF – human splicing finder; MaxEntScan – maximum entropy model; WT – wild type; MUT – mutant.
The score variation difference between wild type and mutation of more than 10 % for HSF and 30 % for MaxEntScan and NNSPLICE was considered as resulting in a splicing defect.

don introduction after incorporation of 25 amino acids; p.Val306Alafs*26. The variant c.1183+1G>T led to skipping of exon 12 (Fig. 2C), and the predicted effect on the protein was disruption of the stop codon and incorporation of additional 126 amino acids, with extension of the protein by 51 residues; p.Pro346Aspfs*130.

None of the detected variants were found in Czech control chromosomes and in the gnomAD v2.1. dataset except for the c.622C>T; p.(Arg208Trp) present in one allele out of 251,466.

Clinical data

A summary of the clinical data is provided in Table 4. BCVA was reduced in all affected subjects, ranging from 0.5 to light perception. Individual IV:1 from Family 6 and his son IV:4 (Fig. 1) had lost vision in one

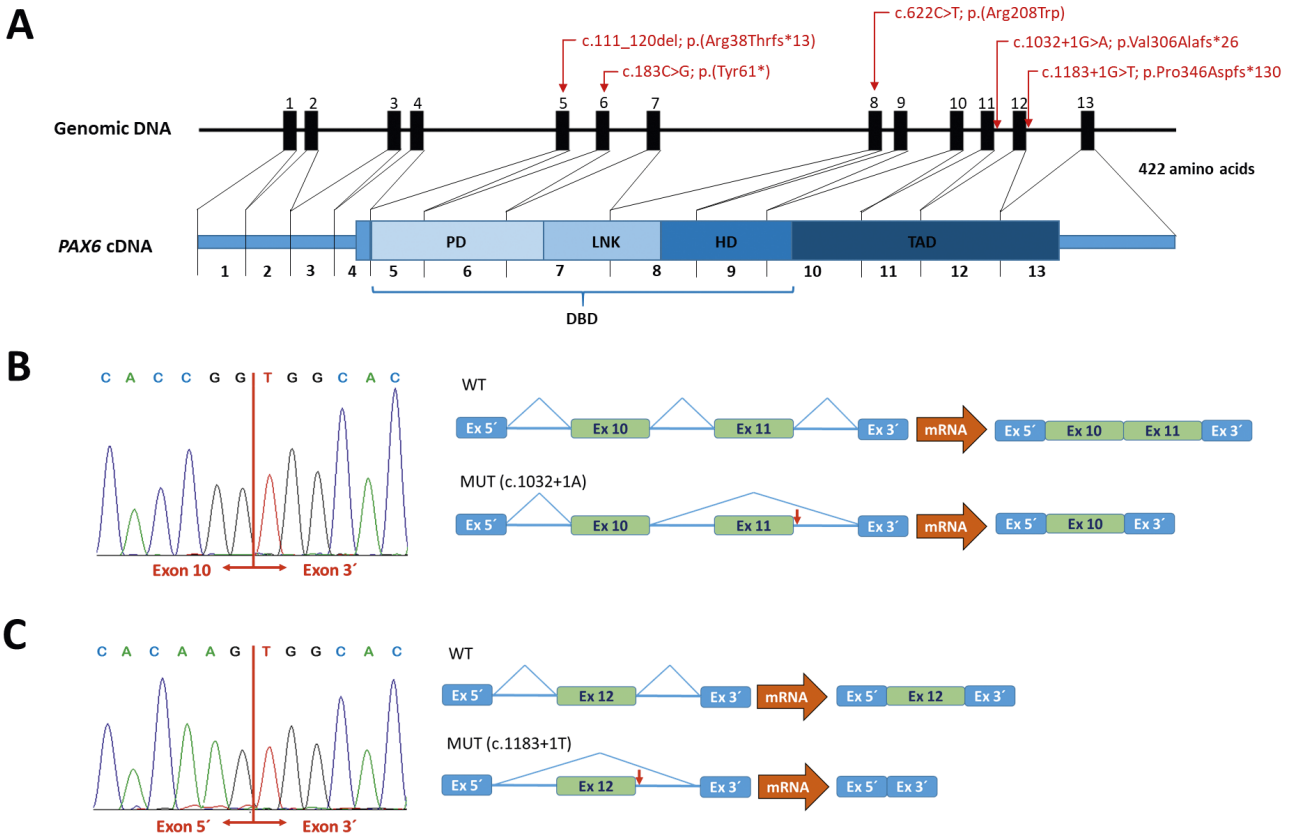

Fig. 2. Overview of identified variants in the *PAX6* gene and functional analysis using the exon trapping assay
(**A**) Structures of human *PAX6* gene/cDNA, domains and variants found. DBD – DNA-binding domain; PD – paired domain; LNK – linker region; HD – homeodomain; TAD – transactivation domain. (**B**) Sequence chromatogram of cDNA derived from mutant allele c.1032+1A and schematic splicing model of the wild-type (WT) and mutant (MUT) allele. Note skipping of exon 11 for the mutant allele as only the sequence from exon 10 and vector-derived exons was obtained. (**C**) Sequence chromatogram of cDNA derived from mutant allele c.1183+1T and schematic splicing model of the wild-type and mutant allele. The disease-causing variant leads to exon 12 skipping as only the sequence from the vector-derived exons was obtained.

Table 4. Clinical findings of 11 individuals with an aniridia spectrum disorder

	BCVA		Ocular findings		Ocular surgery	
ID/age	**RE**	**LE**	**RE**	**LE**	**RE**	**LE**
F1-II:4/50	0.02	LP	Nystagmus, complete aniridia, macular hypoplasia, glaucoma since 18 y	Nystagmus, complete aniridia, glaucoma since 18 y, phthisis, fundus examination not possible	Cataract extraction at 18 y, TE at 42 y	Cataract extraction at 15 y, secondary IOL implantation at 38 y, PPV at 40 y, IOL explantation at 41 y, TE at 41 y, PK at 45 y, rePK at 49 y
F1-III:5/27	LP	LP	Nystagmus, partial aniridia, macular hypoplasia, glaucoma since 9 y	Nystagmus, partial aniridia, macular hypoplasia, glaucoma since 9 y, fundus examination not possible	Cataract extraction + IOL at 18 y, CPC at 22 y	Cataract extraction + IOL at 17 y CPC at 25 y
F2-II:1/31	0.5	0.5	Mild ptosis, complete aniridia, anterior and posterior subcapsular cataract, mild foveal hypoplasia	Partial aniridia, posterior subcapsular cataract, mild foveal hypoplasia	Cataract extraction + IOL + hydrogel iris implant at 31 y	Cataract extraction + IOL at 30 y
F3-II:1/32	0.1	HM	Nystagmus, microcornea (⌀8 mm), partial aniridia, chorioretinal coloboma	Nystagmus, microcornea (⌀6 mm), partial aniridia, chorioretinal coloboma	Cataract extraction at 9 y	Cataract extraction at 10 y
F4-II:2/8	0.3	0.4	High myopia (−14 D), nystagmus, anterior polar cataract, optic nerve coloboma, mild foveal hypoplasia	High myopia (−15 D), nystagmus, anterior polar cataract, optic nerve coloboma, mild foveal hypoplasia	Nil	Nil
F5-II:2/46	0.01	0.01	Severe ptosis, nystagmus, fibrovascular pannus, partial aniridia, anterior polar cataract, foveal hypoplasia, glaucoma since 42 y	Severe ptosis, nystagmus, fibrovascular pannus, iris hypoplasia, anterior polar cataract, foveal hypoplasia	Cataract extraction + IOL at 44 y	Cataract extraction + PPV at 45 y, IOL at 46 y
F5-III:2/11	0.2	0.2	Nystagmus, embryotoxon, peripheral keratopathy, complete aniridia, foveal hypoplasia	Nystagmus, embryotoxon, peripheral keratopathy, complete aniridia, foveal hypoplasia	Nil	Nil
F6-III:1/46	0	0.2	Nystagmus, band keratopathy, complete aniridia, post-traumatic phthisis	Nystagmus, complete aniridia, nuclear cataract, foveal hypoplasia, glaucoma	Nil	Nil
F6-IV:4/20	0.02	0	Nystagmus, complete aniridia, chorioretinal coloboma, foveal hypoplasia, glaucoma since 13 y	Nystagmus, complete aniridia, chorioretinal coloboma in documentation, post-traumatic phthisis	Cataract extraction in childhood, cyclocryotherapy at 18 y	Cataract extraction in childhood
F6-IV:5/16	0.15	0.15	Nystagmus, complete aniridia, peripheral keratopathy, glaucoma since 16 y	Nystagmus, complete aniridia, peripheral keratopathy, glaucoma since 16 y	Nil	Nil
F6-IV:6/15	0.1	0.1	Nystagmus, complete aniridia, anterior polar cataract, chorioretinal coloboma, foveal hypoplasia	Nystagmus, complete aniridia, anterior polar cataract, chorioretinal coloboma, foveal hypoplasia	Nil	Nil

Abbreviations: CPC – cyclophotocoagulation; D – dioptre; HM – hand movement; LP – light perception; IOL – intraocular lens; PK – penetrating keratoplasty; rePK – repeated penetrating keratoplasty; PPV – pars plana vitrectomy; TE – trabeculectomy; y – year.

eye, reportedly because of trauma. Total absence of the iris was observed in 13 out of the 22 eyes examined. Congenital or childhood onset cataracts were noted in nine patients. Secondary glaucoma was diagnosed in three individuals. One of the affected subjects had bilateral high myopia but no iris defects (Table 4).

Of particular note were clinical findings in four individuals. The proband from Family 2 (Fig. 3A-D), aged 32 years at the last examination, had mild congenital ptosis in the right eye (RE, Fig. 3A) and premature cataract formation in both eyes. Clinical notes at 6 years of age already documented anterior polar and cortical cataract in the RE and cortical cataract in the left eye (LE). She did not have nystagmus and had only mild foveal hypoplasia on SD-OCT (Fig. 3B). She underwent cataract surgery in the LE at the age of 30, and right cataract surgery at the age of 31, during which a hydrogel iris prosthesis (Noviris, Wilens, Prague, Czech Republic) was inserted (Fig. 3C). After surgery, the patient reported reduced photophobia and ocular discomfort. At the

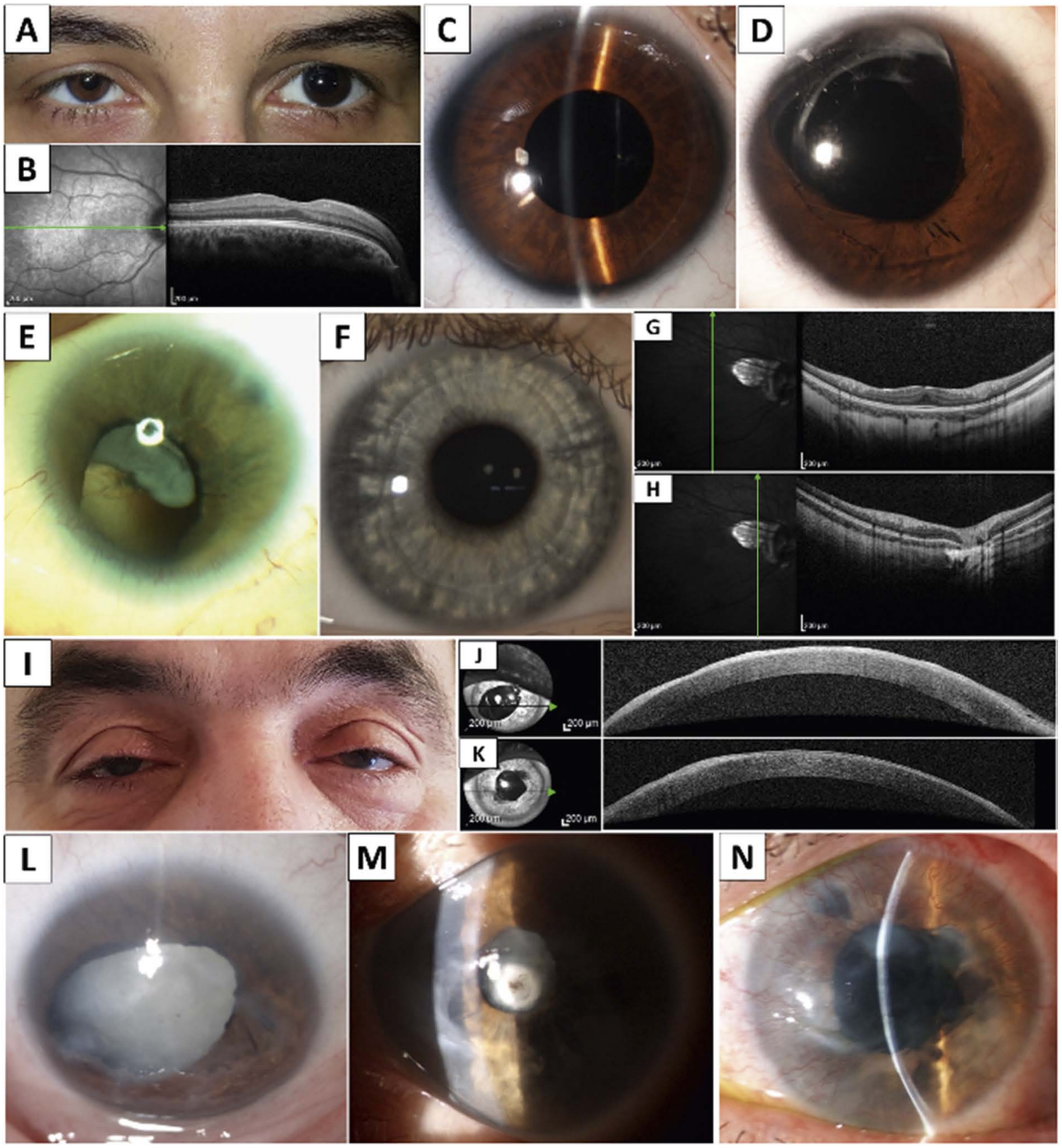

Fig. 3. Spectrum of aniridia phenotypes observed in Czech patients
(**A**) Unilateral ptosis. **(B)** SD-OCT cross-sectional image of the right fovea documenting mild foveal hypoplasia. **(C)** Hydrogel iris prothesis in the RE and (**D**) iris hypoplasia with large coloboma and intraocular lens in the LE in individual II:1 from Family 2 (age 32). (**E**) Microcornea, iris hypoplasia and coloboma with remnants of lens material in the LE of individual II:1 from Family 3 (age 31). **(F)** Anterior polar cataract; note normally appearing iris. **(G)** SD-OCT cross-sectional image documenting mild foveal hypoplasia, and (**H**) optic nerve coloboma in the RE of individual II:1 from Family 4 (age 8). (**I**) Bilateral congenital ptosis in individual II:2 from Family 5 (age 46 years), SD-OCT anterior segment clinical findings in the RE (**J**) and LE (**K**), partial aniridia and cataract in the RE (**L**). **(M)** Iris hypoplasia and anterior polar cataract in the LE in the same patient (age 44) and (**N**) keratopathy with superficial fibrovascular pannus extending from the limbus and vascularization in the LE (age 46).

last follow-up visit, 1.5 years after the procedure, no complications were present.

The index case from Family 3, aged 31 years at the last examination, had bilateral microcornea (Fig. 3E), cataracts requiring surgery in childhood, and iris and chorioretinal colobomas.

The proband from Family 4 was noted since infancy to suffer from progressive high myopia. His refractive error at the age of 7 years was -14 and -15 dioptre sphere in the RE and LE, respectively. Anterior polar cataracts not requiring surgical intervention and very mild nystagmus were also noted. He did not have any iris defects (Fig. 3F), and only mild transillumination around the pupils was noted. Examination of the posterior pole showed small optic nerve colobomas and mild foveal hypoplasia (Fig. 3G,H).

The proband from Family 5 (individual II:3, Fig. 1), aged 46 years, had nystagmus, bilateral severe congenital ptosis (Fig. 3I), partial aniridia in the RE and iris hypoplasia in the LE (Fig. 3L,M). Bilateral anterior polar cataracts (Fig. 3D) were described in the clinical notes when he was 32 years old, eventually progressing into dense corticonuclear opacity (Fig. 3C) requiring cataract surgery at the age of 44 and 45 years, in the RE and LE, respectively. The patient also suffered from marked bilateral keratopathy with fibrovascular pannus (Fig. 3E,F,G). Bilateral foveal hypoplasia was confirmed by SD-OCT. Systemic findings included impaired glucose tolerance, hepatopathy of unknown origin, and thrombocytopenia. His daughter (individual III:2, Fig. 1), aged 11 years, had classical aniridia with total bilateral absence of the iris, clear lenses and no ptosis.

Two siblings (individuals IV:4, IV:5, from Family 6) were reported by the parent to have learning difficulties; further evaluation, however, was not possible.

Discussion

Sequence variants in *PAX6* have been recognized as the genetic cause of aniridia for more than two decades (Jordan et al., 1992). In this study we identified disease-causing variants in six families of Czech origin, of which two were novel, and performed functional analysis of two *PAX6* variants using a minigene strategy. We also show in detail the associated phenotypes, with particular emphasis on the features rarely observed in patients with *PAX6* disease-causing mutations.

As *PAX6* is actively transcribed in tissues forming the eye (i.e., lens, retina, cornea, iris, trabecular meshwork and lacrimal gland), forebrain and hindbrain/cerebellum, spinal cord, pancreas and pituitary (Ypsilanti and Rubenstein, 2016), the functional impact of the identified changes on splicing is difficult to be assessed using patient-derived tissue. We therefore performed an exon trapping assay using minigenes assembled in the Exontrap vector pET01 and demonstrated that the c.1032+1G>A and c.1183+1G>T variants disrupt normal splicing of *PAX6,* most likely triggering mRNA degradation via the nonsense-mediated decay (NMD) mechanism or nonstop decay with subsequent haploinsufficiency (Byers, 2002; Kong and Liebhaber, 2007). NMD is also expected to be employed in Family 1 with p.(Arg38Thrfs*13) and Family 2 with p.(Tyr61*); while the amino acid substitution p.(Arg208Trp) in Families 3 and 4 located in a highly conserved homeodomain in the nuclear localization sequence (Fig. 2A) may impair transport of *PAX6* to the nucleus (Ploski et al., 2004).

Approximately one third of aniridia cases appear to be *de novo* (Prosser and van Heyningen, 1998). In the current study, three probands out of six had no family history of disease. The *de novo* origin was further supported in two of these families by paternity testing.

In addition to the common phenotypic features in patients with *PAX6* variants, such as partial or complete aniridia and foveal hypoplasia, we also observed some rare findings. The clinical phenotype of individual II:1 from Family 5 supported the previous observation that the combination of congenital ptosis, iris hypoplasia, anterior polar cataracts, fibrovascular pannus and impaired glucose tolerance may be a distinct phenotypic subtype of *PAX6*-associated disease (Peter et al., 2013). However, as the daughter carrying the same pathogenic *PAX6* variant had typical aniridia with no ptosis, other environmental or genetic factors are likely to be involved in the pathogenesis. Nevertheless, an additional case with impaired glucose tolerance supports glycaemic monitoring to become a clinical standard in aniridia management.

In the proband from Family 3, bilateral microcornea and posterior segment colobomas were found, which are also rare findings in patients with *PAX6* variants. For example, Wang et al. (2012) found microcornea in only four probands out of 35 (11.4 %), and in a recently reported family carrying the same variant, three out of 19 (15.7 %) affected members had microcornea (Goolam et al., 2018).

Interestingly, the proband from Family 4 shown to carry the same mutation as proband from Family 3 was regarded as a case with high myopia and anterior polar cataracts. Aniridia spectrum disorder had not been suspected until molecular genetic investigation was undertaken. The c.622C>T variant detected in this individual can be found in one individual in the gnomAD dataset, highlighting the potential for a mild phenotype associated with this particular variant, which is in line with the fact that its effect at the protein level is predicted to be a missense change, possibly hypomorphic, not leading to haploinsufficiency like variants causing classical aniridia (Williamson et al., 2020). Except for our study, the p.(Arg208Trp) variant has been previously observed in several families with members exhibiting both classical and typical phenotypes (Hanson et al., 1993; Lim et al., 2012; Goolam et al., 2018).

A possible association of *PAX6* variants and cognitive deficiency has been reported (Ton et al., 1991; Chien et al., 2009). Two individuals from our series were found to have severe learning difficulties. Unfortunately, further investigation was not possible.

The limitations and benefits of artificial iris implantation in patients with aniridia have been debated (Mostafa et al., 2018). The proband from Family 2 had undergone this type of surgery in her RE with a very satisfactory cosmetic and subjective outcome. It should be, however, noted that the patient had a relatively mild aniridia phenotype with no nystagmus, keratopathy or glaucoma.

In summary, our study identified two novel *PAX6* disease-causing variants and confirmed that the associated phenotypic spectrum is very broad, including high myopia with anterior polar cataracts but no iris defects, or congenital ptosis with anterior polar cataracts and progressive corneal opacification in adulthood, variably associated with impaired glucose tolerance.

Acknowledgements

The authors are grateful to Martin Meliska for providing the SD-OCT examination of patients. This work has been generated within the European Reference Network for Rare Eye Diseases (ERN-EYE).

References

Byers, P. H. (2002) Killing the messenger: new insights into nonsense-mediated mRNA decay. *J. Clin. Invest.* **109**, 3-6.

Chien, Y. H., Huang, H. P., Hwu, W. L., Chien, Y. H., Chang, T. C., Lee, N. C. (2009) Eye anomalies and neurological manifestations in patients with PAX6 mutations. *Mol. Vis.* **15**, 2139-2145.

Dansault, A., David, G., Schwartz, C., Jaliffa, C., Vieira, V., de la Houssaye, G., Bigot, K., Catin, F., Tattu, L., Chopin, C., Halimi, P., Roche, O., Van Regemorter, N., Munier, F., Schorderet, D., Dufier, J. L., Marsac, C., Ricquier, D., Menasche, M., Penfornis, A., Abitbol, M. (2007) Three new PAX6 mutations including one causing an unusual ophthalmic phenotype associated with neurodevelopmental abnormalities. *Mol. Vis.* **13**, 511-523.

Goolam, S., Carstens, N., Ross, M., Bentley, D., Lopes, M., Peden, J., Kingsbury, Z., Tsogka, E., Barlow, R., Carmichael, T. R., Ramsay, M., Williams, S. E. (2018) Familial congenital cataract, coloboma, and nystagmus phenotype with variable expression caused by mutation in PAX6 in a South African family. *Mol. Vis.* **24**, 407-413.

Graziano, C., D'Elia, A. V., Mazzanti, L., Moscano, F., Guidelli Guidi, S., Scarano, E., Turchetti, D., Franzoni, E., Romeo, G., Damante, G., Seri, M. (2007) A de novo nonsense mutation of PAX6 gene in a patient with aniridia, ataxia, and mental retardation. *Am. J. Med. Genet. A* **143A**, 1802-1805.

Grindley, J. C., Davidson, D. R., Hill, R. E. (1995) The role of Pax-6 in eye and nasal development. *Development* **121**, 1433-1442.

Gronskov, K., Rosenberg, T., Sand, A., Brondum-Nielsen, K. (1999) Mutational analysis of PAX6: 16 novel mutations including 5 missense mutations with a mild aniridia phenotype. *Eur. J. Hum. Genet.* **7**, 274-286.

Gronskov, K., Olsen, J. H., Sand, A., Pedersen, W., Carlsen, N., Bak Jylling, A. M., Lyngbye, T., Brondum-Nielsen, K., Rosenberg, T. (2001) Population-based risk estimates of Wilms tumour in sporadic aniridia. A comprehensive mutation screening procedure of PAX6 identifies 80% of mutations in aniridia. *Hum. Genet.* **109**, 11-18.

Hanson, I. M., Seawright, A., Hardman, K., Hodgson, S., Zaletayev, D., Fekete, G., van Heyningen, V. (1993) PAX6 mutations in aniridia. *Hum. Mol. Genet.* **2**, 915-920.

Hanson, I., Van Heyningen, V. (1995) Pax6: more than meets the eye. *Trends Genet.* **11**, 268-272.

Hewitt, A. W., Kearns, L. S., Jamieson, R. V., Williamson, K. A., van Heyningen, V., Mackey, D. A. (2007) PAX6 mutations may be associated with high myopia. *Ophthalmic Genet.* **28**, 179-182.

Hingorani, M., Williamson, K. A., Moore, A. T., van Heyningen, V. (2009) Detailed ophthalmologic evaluation of 43 individuals with PAX6 mutations. *Invest. Ophthalmol. Vis. Sci.* **50**, 2581-2590.

Jin, C., Wang, Q., Li, J., Zhu, Y., Shentu, X., Yao, K. (2012) A recurrent PAX6 mutation is associated with aniridia and congenital progressive cataract in a Chinese family. *Mol. Vis.* **18**, 465-470.

Jordan, T., Hanson, I., Zaletayev, D., Hodgson, S., Prosser, J., Seawright, A., Hastie, N., van Heyningen, V. (1992) The human PAX6 gene is mutated in two patients with aniridia. *Nat. Genet.* **1**, 328-332.

Karczewski, K. J., Francioli, L. C., Tiao, G., Cummings, B. B., Alfoldi, J., Wang, Q., Collins, R. L., Laricchia, K. M., Ganna, A., Birnbaum, D. P., Gauthier, L. D., Brand, H., Solomonson, M., Watts, N. A., Rhodes, D., Singer-Berk, M., England, E. M., Seaby, E. G., Kosmicki, J. A., Walters, R. K., Tashman, K., Farjoun, Y., Banks, E., Poterba, T., Wang, A., Seed, C., Whiffin, N., Chong, J. X., Samocha, K. E., Pierce-Hoffman, E., Zappala, Z., O'Donnell-Luria, A. H., Minikel, E. V., Weisburd, B., Lek, M., Ware, J. S., Vittal, C., Armean, I. M., Bergelson, L., Cibulskis, K., Connolly, K. M., Covarrubias, M., Donnelly, S., Ferriera, S., Gabriel, S., Gentry, J., Gupta, N., Jeandet, T., Kaplan, D., Llanwarne, C., Munshi, R., Novod, S., Petrillo, N., Roazen, D., Ruano-Rubio, V., Saltzman, A., Schleicher, M., Soto, J., Tibbetts, K., Tolonen, C., Wade, G., Talkowski, M. E., Genome Aggregation Database, C., Neale, B. M., Daly, M. J., MacArthur, D. G. (2020) The mutational constraint spectrum quantified from variation in 141,456 humans. *Nature* **581**, 434-443.

Kleinberger, J., Maloney, K. A., Pollin, T. I., Jeng, L. J. (2016) An openly available online tool for implementing the ACMG/AMP standards and guidelines for the interpretation of sequence variants. *Genet. Med.* **18**, 1165.

Kong, J., Liebhaber, S. A. (2007) A cell type-restricted mRNA surveillance pathway triggered by ribosome extension into the 3' untranslated region. *Nat. Struct. Mol. Biol.* **14**, 670-676.

Li, H., Durbin, R. (2009) Fast and accurate short read alignment with Burrows-Wheeler transform. *Bioinformatics* **25**, 1754-1760.

Lim, H. T., Seo, E. J., Kim, G. H., Ahn, H., Lee, H. J., Shin, K. H., Lee, J. K., Yoo, H. W. (2012) Comparison between aniridia with and without PAX6 mutations: clinical and molecular analysis in 14 Korean patients with aniridia. *Ophthalmology* **119**, 1258-1264.

Lim, H. T., Kim, D. H., Kim, H. (2017) PAX6 aniridia syndrome: clinics, genetics, and therapeutics. *Curr. Opin. Ophthalmol.* **28**, 436-447.

Malandrini, A., Mari, F., Palmeri, S., Gambelli, S., Berti, G., Bruttini, M., Bardelli, A. M., Williamson, K., van Heyningen, V., Renieri, A. (2001) PAX6 mutation in a family with aniridia, congenital ptosis, and mental retardation. *Clin. Genet.* **60**, 151-154.

Mayer, K. L., Nordlund, M. L., Schwartz, G. S., Holland, E. J. (2003) Keratopathy in congenital aniridia. *Ocul. Surf.* **1**, 74-79.

McKenna, A., Hanna, M., Banks, E., Sivachenko, A., Cibulskis, K., Kernytsky, A., Garimella, K., Altshuler, D., Gabriel, S., Daly, M., DePristo, M. A. (2010) The Genome Analysis Toolkit: a MapReduce framework for analyzing next-generation DNA sequencing data. *Genome Res,* **20**, 1297-1303.

Miller, R. W., Fraumeni, J. F., Jr., Manning, M. D. (1964) Association of Wilms's tumor with aniridia, hemihypertrophy and other congenital malformations. *N. Engl. J. Med.* **270**, 922-927.

Miyake, M., Yamashiro, K., Nakanishi, H., Nakata, I., Akagi-Kurashige, Y., Tsujikawa, A., Moriyama, M., Ohno-Matsui, K., Mochizuki, M., Yamada, R., Matsuda, F., Yoshimura, N. (2012) Association of paired box 6 with high myopia in Japanese. *Mol. Vis.* **18,** 2726-2735.

Mostafa, Y. S., Osman, A. A., Hassanein, D. H., Zeid, A. M., Sherif, A. M. (2018) Iris reconstruction using artificial iris prosthesis for management of aniridia. *Eur. J. Ophthalmol.* **28**, 103-107.

Netland, P. A., Scott, M. L., Boyle, J. W. 4th, Lauderdale, J. D. (2011) Ocular and systemic findings in a survey of aniridia subjects. *J. AAPOS* **15**, 562-566.

Perez-Solorzano, S., Chacon-Camacho, O. F., Astiazaran, M. C., Ledesma-Gil, G., Zenteno, J. C. (2017) PAX6 allelic heterogeneity in Mexican congenital aniridia patients: expanding the mutational spectrum with seven novel pathogenic variants. *Clin. Exp. Ophthalmol.* **45**, 875-883.

Peter, N. M., Leyland, M., Mudhar, H. S., Lowndes, J., Owen, K. R., Stewart, H. (2013) PAX6 mutation in association with ptosis, cataract, iris hypoplasia, corneal opacification and diabetes: a new variant of familial aniridia? *Clin. Exp. Ophthalmol.* **41**, 835-841.

Ploski, J. E., Shamsher, M. K., Radu, A. (2004) Paired-type homeodomain transcription factors are imported into the nucleus by karyopherin 13. *Mol. Cell. Biol.* **24**, 4824-4834.

Prosser, J., van Heyningen, V. (1998) PAX6 mutations reviewed. *Hum. Mutat.* **11**, 93-108.

Richards, S., Aziz, N., Bale, S., Bick, D., Das, S., Gastier-Foster, J., Grody, W. W., Hegde, M., Lyon, E., Spector, E., Voelkerding, K., Rehm, H. L., ACMG Laboratory Quality Assurance Committee (2015) Standards and guidelines for the interpretation of sequence variants: a joint consensus recommendation of the American College of Medical Genetics and Genomics and the Association for Molecular Pathology. *Genet. Med.* **17**, 405-424.

Robinson, D. O., Howarth, R. J., Williamson, K. A., van Heyningen, V., Beal, S. J., Crolla, J. A. (2008) Genetic analysis of chromosome 11p13 and the PAX6 gene in a series of 125 cases referred with aniridia. *Am. J. Med. Genet. A* **146A**, 558-569.

Samant, M., Chauhan, B. K., Lathrop, K. L., Nischal, K. K. (2016) Congenital aniridia: etiology, manifestations and management. *Expert Rev. Ophthalmol.* **11**, 135-144.

Ton, C. C., Hirvonen, H., Miwa, H., Weil, M. M., Monaghan, P., Jordan, T., van Heyningen, V., Hastie, N. D., Meijers-Heijboer, H., Drechsler, M., Royer-Pokora, B., Collins, F., Swaroop, A., Strong, L. C., Saunders, G. F. (1991) Positional cloning and characterization of a paired box- and homeobox-containing gene from the aniridia region. *Cell* **67**, 1059-1074.

Valenzuela, A., Cline, R. A. (2004) Ocular and nonocular findings in patients with aniridia. *Can. J. Ophthalmol.* **39**, 632-638.

Wang, K., Li, M., Hakonarson, H. (2010) ANNOVAR: functional annotation of genetic variants from high-throughput sequencing data. *Nucleic Acids Res.* **38**, e164.

Wang, P., Sun, W., Li, S., Xiao, X., Guo, X., Zhang, Q. (2012) PAX6 mutations identified in 4 of 35 families with microcornea. *Invest. Ophthalmol. Vis. Sci.* **53**, 6338-6342.

Williamson, K. A., Hall, H. N., Owen, L. J., Livesey, B. J., Hanson, I. M., Adams, G. G. W., Bodek, S., Calvas, P., Castle, B., Clarke, M., Deng, A. T., Edery, P., Fisher, R., Gillessen-Kaesbach, G., Heon, E., Hurst, J., Josifova, D., Lorenz, B., McKee, S., Meire, F., Moore, A. T., Parker, M., Reiff, C. M., Self, J., Tobias, E. S., Verheij, J., Willems, M., Williams, D., van Heyningen, V., Marsh, J. A., FitzPatrick, D. R. (2020) Recurrent heterozygous PAX6 missense variants cause severe bilateral microphthalmia via predictable effects on DNA-protein interaction. *Genet. Med.* **22**, 598-609.

Ypsilanti, A. R., Rubenstein, J. L. (2016) Transcriptional and epigenetic mechanisms of early cortical development: An examination of how Pax6 coordinates cortical development. *J. Comp. Neurol.* **524**, 609-629.